rNets: A standalone package to visualize reaction networks.

Sergio Pablo-García[1,2,3,*], Raúl Pérez-Soto[4], Albert Sabadell-Rendón[5], Diego Garay-Ruiz[5], Vladyslav Nosylevskyi[6], and Núria López[5]

[1]Department of Chemistry, University of Toronto, Lash Miller Chemical Laboratories 80 St. George Street, ON M5S 3H6, Toronto, Canada
[2]Department of Computer Science, University of Toronto, Sandford Fleming Building, 40 St. George Street, ON M5S 2E4, Toronto, Canada
[3]Vector Institute for Artificial Intelligence, 661 University Ave. Suite 710, ON M5G 1M1, Toronto, Canada
[4]Department of Chemistry, Colorado State University, 1301 Center Avenue, Ft. Collins, CO 80523-1872
[5]Institute of Chemical Research of Catalonia, The Barcelona Institute of Science and Technology, Av. Països Catalans 16, 43007, Tarragona, Spain
[6]Independent Researcher
[*]Corresponding authors email: spgarcica@gmail.com

April 2, 2024

1

Abstract

In the study of chemical reactions, visualizing reaction networks is pivotal for identifying crucial compounds and reactions. Traditional methods, such as network schematics and reaction path linear plots, often struggle to effectively represent complex reaction networks due to their size and intricate connectivity. Alternatives capable of leading with complexity include graph methods, but they are not user-friendly, lacking simplicity and modularity, which hinders their integration with widely-used research software. This work introduces **rNets** an innovative tool designed for the efficient visualization of reaction networks with a user-friendly interface, modularity, and seamless integration with existing software packages. The effectiveness of rNets is demonstrated through its application in analyzing three catalytic reactions, showcasing its potential to significantly enhance research both in homogeneous and heterogeneous catalysis fields. This tool not only simplifies the visualization process but also opens new avenues for exploring complex reaction networks in diverse research contexts.

1 Introduction

Catalyst development plays a pivotal role in enhancing industrial chemical production by optimizing processes to reduce material, financial, and environmental costs [1, 2]. The conventional approach to developing these catalysts relies on a labor-intensive cycle of design, making, and testing of numerous candidates to find the most effective ones for specific reactions. As the number of candidates grows, this method becomes increasingly time-consuming and resource-intensive [2–9]. With pressing environmental challenges, the need for more efficient strategies is evident, prompting the integration of density functional theory (DFT) simulations into the discovery process. DFT simulations offer valuable theoretical insights, acting as a decision-making tool to predict reactions' outcomes more accurately [10–18]. However, effectively utilizing these insights requires not only prediction but also the visualization of the complex networks formed by reactions, a significant challenge in both homogeneous and heterogeneous catalysis due to their branched and complex nature. [19–21].

Traditional visualization techniques, such as reaction path plots, leverage ab-initio data to provide a two-dimensional view of the network's thermodynamics and, when including activation energies, its kinetic behavior. While effective for small, straightforward reactive systems, these plots fall short in representing the intricate, branched networks characteristic of homogeneous and heterogeneous catalysis. This comes as a direct consequence of employing a linear reaction coordinate (step-by-step process) as the x-coordinate of the plot. A more robust alternative is the depiction of reaction mechanisms

3

as reaction network graphs [6, 19, 21], encoding the reaction intermediates as nodes and the reactions which interconnect them, as edges. More specifically, reaction networks are formed by elementary reactions, which are chemical transformations in which one or more reactants evolve into products in a single reaction step [1].

This conceptualization of chemical processes is shared not only by both homogeneous and heterogeneous catalysis [6], but also by any non-catalytic cascade of chemical reactions. Typically, these more complex networks have been illustrated through manually drawn graphs, tracing the reaction mechanism, as depicted in the left part of **Figure 1**. The most used tools to trace these reaction mechanisms and linear energy diagrams manually are Adobe Illustrator [17, 22], OriginLab [18, 23, 24], Inkscape [15, 25, 26], Matplotlib [27–29], and ChemDraw [10–12, 30], among others. From there, it is possible to switch to a representation that is more akin to graphs in other domains of science, explicitly showing nodes as circles and edges as full connections between them (right side of **Figure 1**), using tools such as Graphviz [31].
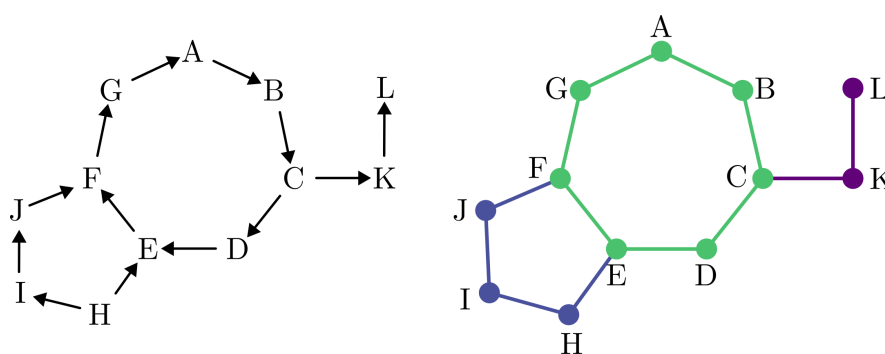

Figure 1: Schematic depictions of a reaction network graph. Left, reaction-centered representation, using reaction arrows to depict processes and labels for intermediates. Right, complete graph-based representation with intermediates as nodes and reactions as edges.

However, this manual approach to graphing reaction mechanisms poses significant limitations. First, the representation cost escalates with the number of compounds, challenging the depiction of networks that suffer from combinatorial explosion [4, 19, 32], which is an increasingly common situation due to the generalization of the use of automated mechanism discovery algorithms [4, 33–44]. Additionally, unlike reaction paths, these graphs do not visually convey thermodynamic and kinetic information. Alternative and promising methods for automatically encoding reactions with these considerations have been proposed [20, 45], but they often face constraints that hinder their widespread adoption by the computational chemistry community, such as being tied to specific software, requiring multiple dependencies, or using complex input formats.

To overcome these limitations, this work introduces a standalone, package-agnostic software designed to efficiently visualize the thermodynamic and kinetic properties of reaction networks, rNets. rNets is built on three core design principles: (i) ease of use for both programmers and non-programmers, (ii) readiness for integration with various DFT and microkinetic (MK) packages, and (iii) minimal dependency requirements to simplify deployment and enhance robustness. To demonstrate the capabilities of our code, we have integrated rNets with two distinct microkinetic modeling packages, showcasing its effectiveness in visualizing the complex reactions associated with both homogeneous and heterogeneous catalysts. Moreover, we have also coupled rNets with a knowledge-graph based representation of reaction networks, integrated within the ioChem-BD [46, 47] database for computational chemistry data. This approach not only streamlines the analysis of intricate

5

catalytic networks but also bridges the gap between theoretical simulations and practical applications, offering a more comprehensive and accessible tool for researchers in the field of computational chemistry. Through rNets, we aim to facilitate a more rapid, automated and informed catalyst discovery process.

2 Methods

rNets, is a software package written in Python 3.12, that aims to provide an extensible and modular tool for visualizing the thermodynamic and kinetic properties of reaction networks. The choice of Python for its development is a nod to the language's widespread use and acceptance within the scientific community. rNets stands out for its ease of use, minimalistic design, and its capability to seamlessly integrate with external codes. The core functionality of rNets involves surrogating the visualization of reaction graphs to Graphviz, a software able to parsing dot files and rendering them in various formats. Thus, rNets can be characterized as a metaprogramming package, able to translate reaction networks into the dot language for visualization, with Graphviz as its sole external dependency. **Figure 2** depicts the logic behind rNets.

However, the rapid development of Python packages for chemistry has been accompanied by increasing complexity in managing software dependencies, a crucial aspect for ensuring consistent and accurate execution of chemical software. Traditional solutions like package managers and virtual environments have only partially addressed these issues, often struggling with
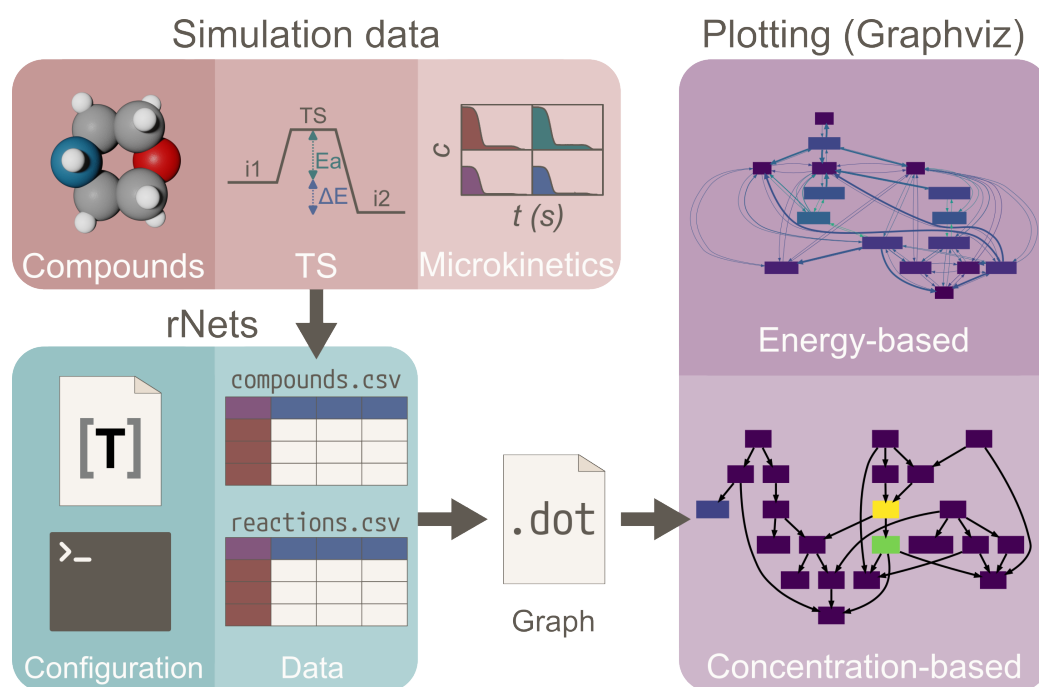
6

Figure 2: Depiction of the workflow followed by rNets. First, the energies of the compounds, transition states and/or concentrations are collected into .csv data files from simulations. Together with the configuration files, rNets is used to generate a .dot file containing the plotting instructions for the graph. Finally, Graphviz is used to compute the energy or concentration-based plot.

the integration of multiple packages that have conflicting dependencies within a single Python distribution. This has resulted in a tendency towards isolated Python packages, each with its own set of dependencies, reducing their modular capabilities. In contrast, rNets has been meticulously crafted as a standalone package, devoid of these dependency entanglements. By requiring only Graphviz for plotting, rNets effectively maximizes its portability and modularity. This strategic design choice, along with its practical implications, are further explored in the following subsections.

7

2.1 Input parsing

Theoretical studies of reaction networks frequently rely on ab-initio methods to compute thermodynamic and kinetic properties, such as ground-state energies of compounds and activation energies of reactions. These properties are typically collated into simple, spreadsheet-like tables for easy parsing and analysis. Reaction path plots, a popular visualization method, excel in depicting these tables, especially for simple mechanisms. Recognizing the simplicity and widespread use of table formats in the research community, rNets has been tailored to interface seamlessly with input files resembling these tables. This design strategy is aimed at facilitating the adoption of rNets, especially among chemists with limited programming expertise. rNets utilizes two primary file types to define a reaction network: the "**compounds**" file, detailing the compounds, and the "**reactions**" file, outlining the reactions. The chosen file format for both is comma-separated values (CSV), balancing simplicity and versatility.

The structure of these files is straightforward: the first line contains column names (in no specific order) that define the data represented in each column, followed by lines that provide the data for individual compounds or reactions. To enhance user flexibility, column names are categorized as either "required" or "optional". The "required" columns constitute the essential data needed to define a compound or a reaction. For instance, the "**compounds**" file mandates the `name` and `energy` columns, whereas the "**reactions**" file requires at least one `cleft` and one `cright` column. During the parsing process, rNets checks for the presence of these required columns in the input

8

files. Conversely, the "optional" columns allow for additional, user-specific customizations to each compound or reaction. This flexibility enables users to tailor the analysis to their specific needs. Tables **Tables S1–S2** summarize this information, offering users a quick reference guide for efficient data organization and input into rNets, also included in the code repository.

2.2 Graphical representation of reaction networks

In rNets, the reaction network extracted from the input files is encoded graphically. This representation involves depicting compounds as nodes and reactions as edges within a graph. The nodes, representing compounds, are illustrated as square boxes, each labeled at the center with the compound's name, derived by default from the "name" column in the "**compounds**" file. To augment the visual appeal and clarity, users have the option to modify the label format using the "optional" `fformat` column in the input file. Here, format modifiers can be applied, separated by a colon (":"). These modifiers include **b** for bold, *i* for italic, and <u>u</u> for underlined text, allowing for a customized and informative visual presentation. Further refining the representation, each edge in the graph symbolizes a reaction connecting two nodes. The default directionality of these reactions is forward, denoted as "->". However, users have the option to alter this directionality to backward ("<-") or bidirectional ("<->") by specifying their preference in the "optional" `direction` column name in the "**reactions**" file. rNets comes with two different graphical encodings: "thermo" representing the thermodynamic values of the compounds and the computed kinetic constants and "kinetic" focusing

9

on the concentrations of the compounds and the net rates of the reactions. These encodings are described in the following sections.

2.2.1 Energy-based representation

This visualization modality extends to the thermodynamic and kinetic aspects of the network. The nodes' background colors signify the thermodynamic energies of compounds, while the fill colors of the directional arrows (depicting reactions) represent the energies of the transition states. Notably, bidirectional reactions are represented by two distinct arrowed edges, effectively illustrating the forward and backward reactions as separate entities. This color encoding is achieved through a normalization process, wherein the minimum and maximum energy values from the superset of compounds and reactions are used to create a function that projects these energies onto the $[0, 1]$ interval. This normalized data is then visually represented using colors from a predefined colorscheme.

rNets is capable of visually encoding reaction kinetics when transition state energies are provided in the "**reactions**" file. These energies, listed under the "optional" `energy` column, enable rNets to dynamically adjust the width of the arrows. This adjustment is proportional to the pseudo-kinetic constants derived from the specified energies, following the methodology outlined in **Note S1**. This feature allows for a more nuanced and informative representation of the reaction network, highlighting the kinetic relationships between different components.

10

2.2.2 Concentration-based representation

In this visualization mode, activated when both concentration (`conc`) and energy (`energy`) metrics are specified for all network entities at a chosen time step, rNets illustrate the reaction dynamics. Node backgrounds depict compound concentrations, using a color gradient normalized for immediate clarity, and arrow widths signify reaction rates—wider arrows indicate faster reactions. Directionality is inherently shown by the net reaction rate, without the need for explicit `direction` markers. This design, with concentration and rate normalization, offers a direct, unified view of the reaction network's kinetics and dynamics at any simulated time step. Normalization of concentration and rate values ensures consistent visualization scales. For detailed computational methods behind these values, see **Note S2**.

2.2.3 Color selection

rNets includes a color utility mode to chose the desired color gradient to represent used to represent the previous representation, being Viridis the default choice [48]. Users can use this utility to define their own colorschemes by defining a simple list of colors, as detailed in **Note S3**. Examples can be found in the **Figure S1**. Additionally, to ensure label readability against varied background colors, the luminance of each node's background is considered, with label colors adjusted accordingly to enhance contrast and legibility, as explained in **Note S4**.

2.3 Enhanced component visibility

rNets incorporates a feature that addresses the common need in reaction network visualization to selectively focus on certain parts of the network. Researchers often find themselves in situations where some compounds or reactions may not be relevant to their current analysis or where highlighting specific segments of the network is desired. However, even when certain elements are not the focus, their energies play a crucial role, especially in representing kinetic properties, and thus cannot be entirely omitted from the dataset. As a solution, rNets introduces the `visible` column functionality. This feature grants users the flexibility to either hide or dim specific compounds or reactions within the graphical depiction of the network. When the `visible` column for a given element is set to `false`, that particular compound or reaction will not appear in the visual representation of the reaction graph. Importantly, this does not remove its influence from the overall network; it continues to contribute to the normalization of network energies. For compounds, this means they are still considered in the computation of kinetic constants for related reactions.

In instances where complete removal of an element from the visual field is not desired, setting the `visible` column to `grey` offers an alternative. This option achromatizes the node or edge associated with the element, effectively making it less prominent without entirely eliminating it from the visual network. This greying out of elements allows for a nuanced approach to visualization, enabling users to de-emphasize certain aspects of the network while maintaining a holistic view.

12

This `visible` column feature in rNets provides a powerful and flexible tool for users, allowing them to tailor the network visualization to their specific research needs. It ensures that the graphical representation of the network remains comprehensive yet clear, focusing on elements of interest without losing sight of the overall context of the network.

2.4 Customization and user interface

rNets equips the users with extensive customization capabilities, allowing for the personalization of network visualizations. Users can adjust different plot options, such as the maximum edge width and color scheme, tailoring the visual output to their preferences. These options can be configured through two primary methods: (i) a TOML file that specifies the desired values, and (ii) direct command-line interface (CLI) arguments for on-the-fly adjustments.

The hierarchical structure of option precedence ensures flexibility and control; settings defined in the configuration file override the default values coded within rNets, while CLI arguments take precedence over both configuration settings and defaults. This design allows users to establish a baseline configuration file reflecting their standard visualization preferences, with the flexibility to use CLI arguments for temporary or experiment-specific modifications. rNets rigorously checks the validity of user-defined values to maintain stability and reliability. The available configuration options are described in **Tables S3–S5** and an example of a configuration file can be found in **Note S5** and in the code repository. For advanced customization, the `opts` option enables the specification of Graphviz parameters for various

13

elements of the network visualization. Additional details on utilizing this feature are available in **Note S6**.

In addition to its standalone functionality, rNets is designed for seamless integration as a Python library within broader Python projects. This capability is comprehensively documented, ensuring users can effectively incorporate rNets into their workflows.

3   Results and discussion

In this section, we are presenting three case studies, tackling both homogeneous and heterogeneous catalysis, to demonstrate the capability and versatility of rNets for solving the aforementioned challenges in this field of study. Further details about the relevant simulation details are available in the Supplementary Information (**Note S7–S9**).

The inspection of the energies of reaction networks provides valuable insights about chemical systems. Indeed, although experimental observations can be correlated to energies, it is challenging to provide a one-to-one mapping with properties such as selectivity, yield, or conversion [10, 49], which are essential to control a given chemical process. In this context, microkinetic simulations are a valuable tool to bridge this gap and allow an actual quantitative comparison with experimental results.

14

3.1 Energy-based examples

3.1.1 Imine condensation

Linear free energy profiles are commonly used in mechanistic studies in homogeneous phase. In this context, the application of energy corrections is a standard practice to mitigate the various limitations associated with DFT simulations [50]. These corrections have different origins, such as reference state [51], quasi-harmonic vibrational [52], single-point (SP) energy, counterpoise-corrections [53] or entropic corrections [54], and are crucial for enhancing the accuracy of DFT predictions. However, as the reaction network's complexity escalates, the task of understanding how these corrections influence the overall reaction process becomes increasingly daunting.

This complexity and the critical role of corrections were exemplified in our previous investigation of imine condensation between benzaldehyde and n-butylamine in aprotic media [55]. In that study we observed how a bias of 13.38 kJ/mol per computed structure coupled with a reference state correction (from 1 atm to 1 M) was able to bridge the gap between the DFT-derived microkinetic simulation and the experimental concentration *vs* time values. The rNets' representation of both, the uncorrected system and the corrected system are included in the SI (**Figure S1**), while a simplified representation is included in **Figure 3**.

The full reaction network is composed of a total of 28 species and 52 reversible reactions, which in its majority corresponds to bimolecular association processes, leading to an intricate network. A preliminary examination of the plot in **Figure 3b** readily reveals two prominent alterations within
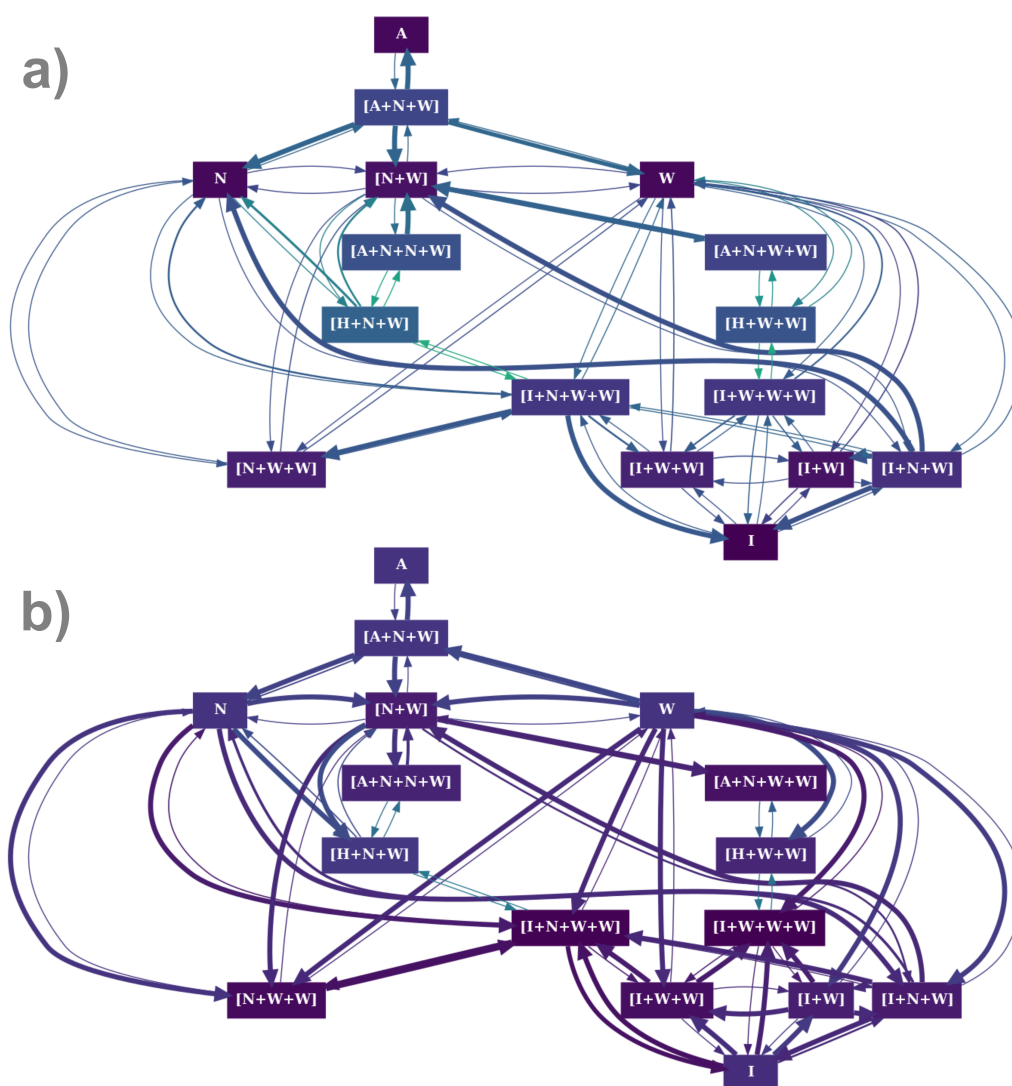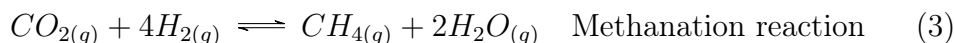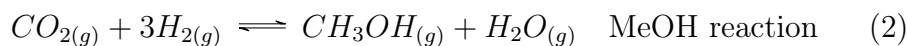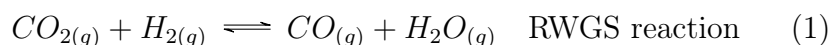
Figure 3: Simplified reaction network of the imine condensation in DCM between benzaldehyde (A) and n-butylamine (N). The adduct of 'X' and 'Y' is represented as '[X+Y]'. Water, the hemiaminal intermediate and the product Imine are represented as 'W', 'H' and 'I' respectively. The magnitude of the energy barriers for each elementary step is represented by the color and the thickness of the arrows, while the color of the nodes represents the stability of the intermediates. The color scale goes from dark, corresponding to low energies (thus high stability) and barriers to light colors, indicating unstable intermediates and high barriers. a) Corresponds reaction network without any correction and b) corresponds to the same network but with standard state correction and a bias of 13.38 kJ/mol per DFT calculation.

16

the network: a notably darker overall tone and an increased presence of thicker edges, indicating significant changes. Further scrutiny of the network highlights specific variations in the appearances of species "A" and "I", which correspond to benzaldehyde and N-butyl-1-phenylmethanimine, respectively. Notably, these species exhibit a lighter shade in **Figure 3b** compared to the rest of the network, suggesting differential effects of the applied corrections on these particular reaction components. The different adducts (i.e. the adduct of "A" and "W" is represented as "[A+W]") have become darker, indicating]that they are now more stable. As a consequence, the overall reaction becomes more dynamic, as the generalized increase in the thickness of the edges indicates. Some reactions are still slow, such as the uncatalyzed hemi-aminal dehydration (corresponding to the edges between "H" and "[I+W]", in green). This interpretation aligns well with the results of the microkinetic simulations carried out in the original work where the simulations with the uncorrected system (**Figure 3a**), led to no imine formation, while the simulations of the corrected system were consistent with previous experimental results.

3.1.2 CO_2 hydrogenation on Pd(111)

Bridging the intricate dynamics observed in the reaction network with broader applications in heterogeneous catalysis, the transition to CO_2 hydrogenation on metal surfaces exemplifies the shift from complex molecular interactions to the activation of small molecules. In this context, reaction paths tend to be considered simple, yet this oversimplified view is challenged even in one of the most appealing reactions. CO_2 hydrogenation on transition metal cat-

17

alysts is the perfect example of an interesting heterogeneous reaction from both academic and industry points of view, as CO_2 is recycled into added-value precursors and products such as CO *via* the reverse water gas shift (RWGS) reaction [56, 57], methanol [24, 56, 57], and methane as side product [15, 56, 58, 59], **Eq. 1–3**. However, even if the number of atoms involved in the potential products is small, the reaction networks include multiple competing pathways, and different kinds of equilibria [19, 26, 56]. Thus, the visualization and posterior analysis of the energy reaction profiles is extremely complex [19, 26]. Consequently, in the reactors, the three equations below take place simultaneously and the extent of each of them depends on the catalyst and operation conditions.

$$CO_{2(g)} + H_{2(g)} \rightleftharpoons CO_{(g)} + H_2O_{(g)} \quad \text{RWGS reaction} \quad (1)$$

$$CO_{2(g)} + 3H_{2(g)} \rightleftharpoons CH_3OH_{(g)} + H_2O_{(g)} \quad \text{MeOH reaction} \quad (2)$$

$$CO_{2(g)} + 4H_{2(g)} \rightleftharpoons CH_{4(g)} + 2H_2O_{(g)} \quad \text{Methanation reaction} \quad (3)$$

In **Figure 4** we report as an example the simplified reaction network of CO_2 hydrogenation on Pd(111) neglecting the formation of methane, involving 21 elementary steps, 16 intermediates, and 5 gas-phase species (labelling at **Table S7**). The network starts with the adsorption and dissociation of H_2 (i1) on the surface (i0). Then, CO_2 is adsorbed (i2), and the reaction evolves through the oxygen hydrogenation of CO_2, resulting in COOH* (i3), leading to the dissociation of i3 into CO* and OH* fragments, and the posterior elimination of OH* *via* water formation and desorption (intermediates i5 and i6) [57, 60]. At this point, the reaction can evolve towards two different path-

18

ways: CO^* desorption (i6 to $CO_{(g)}$ and i0), culminating the RWGS reaction, or CO^* sequential hydrogenation to generate methanol (from i7 to i8 or i13). We use the last elementary steps as examples to understand the information contained in **Figure 4**. The color of the i8 intermediate ($COH^* + H^*$) is brighter than i7 ($CO^* + 2H^*$) meaning that this step is thermodynamically unfavored, as for i13 formation ($CHO^* + H^*$). The kinetic equilibrium between the initial and the final steps is expressed with the thickness and the color of the arrows (edges) in forward or backward directions. Thus, according to **Figure 4**, CO^* hydrogenation pathway is less favored than the RWGS route both thermodynamically and kinetically.

Following the CO^* hydrogenation pathway through $COH^* + H^*$ intermediate (i8), the next step is the generation of $CHOH^*$ (i9). Then, i9 is sequentially hydrogenated to obtain methanol (i12) *via* $CHOH^* + 2H^*$ and $CH_2OH + H^*$ intermediates (i10 and i11 respectively). Alternatively, CO^* can be also hydrogenated through $CHO^* + H^*$ (i13), followed by the generation of CH_2O^*, $CH_2O^* + 2H^*$, and CH_3O^* (i14, i15, and i16 respectively). However, the formation of CH_2O intermediate (i14) is kinetically less probable than $CHOH^*$, and thus, the reaction would evolve through the i9, i10, i11, and i12 pathway according to **Figure 4**. In any case, the formation of COH^* is thermodynamically more favored than CHO^*, since i13 is brighter than i8, and thus, methanol generation is more prone to evolve through the i8 route. All these observations are in line with previous computational and experimental works [18, 57].
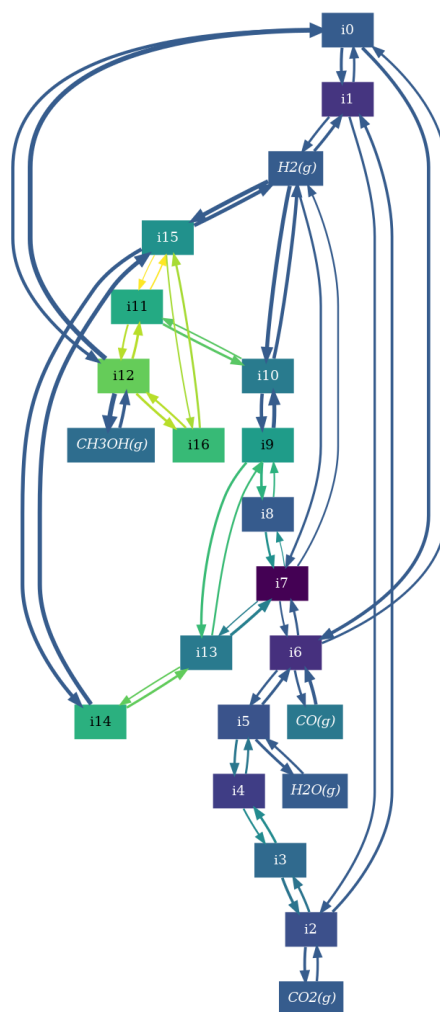
19

Figure 4: Visualization of the reaction network for CO_2 hydrogenation on Pd(111). The intermediates are labeled in **Table S3**. The magnitude of the energy barriers for each elementary step is represented by the color and the thickness of the arrows, while the color of the nodes represent the stability of the intermediates. Bright colors imply unstable intermediates or high activation energies.

20

3.1.3 Networks as knowledge graphs

Having explored the integration of rNets with automation frameworks such as AMUSE, we have established a robust environment for the analysis of reaction networks. The importance of automatic data generation cannot be overstated, yet equally crucial is the adherence to the FAIR (findable, accessible, interoperable, and reusable) principles for data reporting [61]. This balance presents a significant challenge in managing data from computationally characterized reaction networks. Computational chemistry packages generate very heterogeneous output files, for which either manual inspection or the development of specific parsers are essential to retrieve the required information. Because of this, is also common for researchers to only share these properties that have been extracted, thus leaving likely relevant data that has already been computed out of the set of information that is eventually published. Moreover, the definition of the relationships between the chemical entities represented by the finished simulations, e.g., the specification of the chemical reactions taking place in a given reaction network, does also lack a general normalization.

The ioChem-BD platform [46, 47] provides a robust solution for the first part of the problem, translating these diverse output files into an unique format (CML) and providing a framework in which completely curated datasets can be shared with the community, enhancing reproducibility and interoperability. Regarding the relationships between data elements, the OntoRXN ontology [62] was introduced as an organization scheme following the principles of semantic data, which established the core entities that are required to

21

properly define a CRN and map it to the properties gathered from quantum chemical methods. Through the combination of ioChem-BD and OntoRXN, it becomes possible to define *knowledge graphs* (CRN-KGs): non-relational databases which contain all the information about a given reaction network. A CRN-KG, then, can be used as a standard format to process and analyze data, extracting the properties and relationships of interest through queries in the SPARQL format.

One of the foundational applications of CRN-KGs was indeed the automated setup of microkinetic models, processing the individual elementary steps encoded in the knowledge graphs and determining the corresponding reaction barriers and rate constants. In this context, rNets provides a solid foundation to streamline the visualization of the simplified CRN gathered from the CRN-KG and to follow up with the introduction of standards for computational chemical reaction networks. Additionally, we can consider this pipeline as a relatively straightforward connection between rNets and the increasing number of computational results available in ioChem-BD. As a test system, we have consider the halide-catalyzed regiospecific fixation of carbon dioxide in a cyclooctene-based epoxy alcohol [63], for which the results of microkinetic simulations were in very good agreement with experimental yields and selectivities. Despite its simplicity in species and reactions, this system offers a practical example for kinetic simulations in homogeneous catalysis and reveals unique mechanistic insights due to the cyclooctene moiety's versatility.

A naive direct application of rNets to this mechanism resulted in a reaction network that was challenging to interpret, as depicted in **Figure S2**.
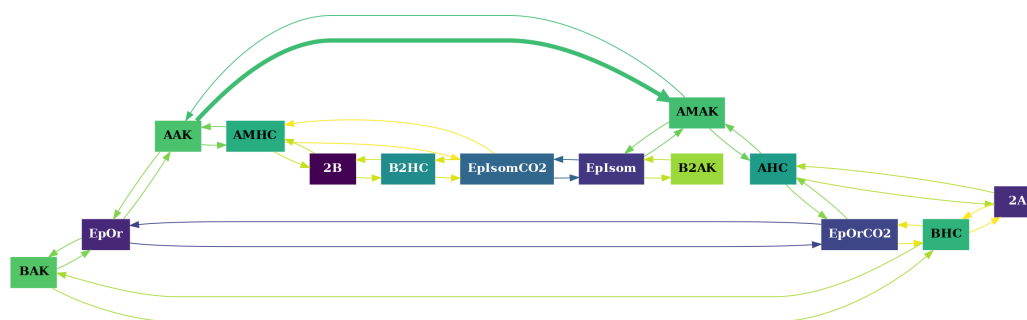
22

Figure 5: Visualization of the reaction network for CO_2 fixation on a epoxy alcohol cyclooctene derivative. The magnitude of the energy barriers for each elementary step is represented by the color and the thickness of the arrows, while the color of the nodes represents the stability of the intermediates.

This complexity arose from modeling most chemical reaction network (CRN) processes as transitions from bimolecular reactants to bimolecular products, which often resulted in the mapping of two nodes to another pair of nodes, cluttering the visual representation with numerous arrows. This scenario, however, showcases the ideal context for demonstrating the visualization enhancement capabilities of rNets. While some of the species in the network (namely, the counterion TMA, the bromide salt TMABr and carbon dioxide) are required to balance energies and appropriately compute barriers and rate constants, they might be omitted from the reaction network in order to focus on the actual rearrangement of the epoxy alcohol to the cyclic carbonate and the different pathways through it which might occur. Therefore, setting the `visible` property of these entities to `false` sheerly improves the readability of the produced graph (**Figure 5**), while keeping compound and reaction energies consistent.

These three examples highlight the versatility of rNets to handle the complexity of reaction networks in both homogeneous and heterogeneous cataly-

23

sis, as well as different schemes for data organization. There is a clear synergy between tools for automated data generation (AMUSE), and tools for the standardization of the produced information (ioChem-BD and CRN-KGs). rNets would conform an essential part of this coupled workflow, simplifying and unifying the visualization of the likely very complex systems studied through this kind of pipelines. Furthermore, the possibility of performing microkinetic simulations as part of this workflow opens the door to in-situ visualizations of the evolution of the concentrations of the different species in the reaction network, as we will detail in the following section.

3.2 Concentration-based examples

3.2.1 Reassessing the imine condensation reaction

To showcase the strengths of rNets in illustrating kinetic outcomes, we revisited our earlier imine condensation reaction [55] through the lens of the recently presented "Dynamic Radii Adjustment for Continuum Solvation" (DRACO) [64], aiming to discern the need of the 13.38 kJ/mol correction, potentially prompted by inaccuracies in handling implicit solvation. This inquiry is powered by the use of pykinetic [65], a Python library tailored for the creation and analysis of kinetic models. This approach not only tests the validity of previous findings but also highlights the synergy between advanced simulation tools and kinetic modeling in refining our understanding of chemical processes.

We have followed the same methodology as in our original paper, and recomputed the potential energies through SP simulations using the adjusted

24

radii computed using DRACO. We recomputed the free energies and added a reference state correction from 1 atm to 1 M.
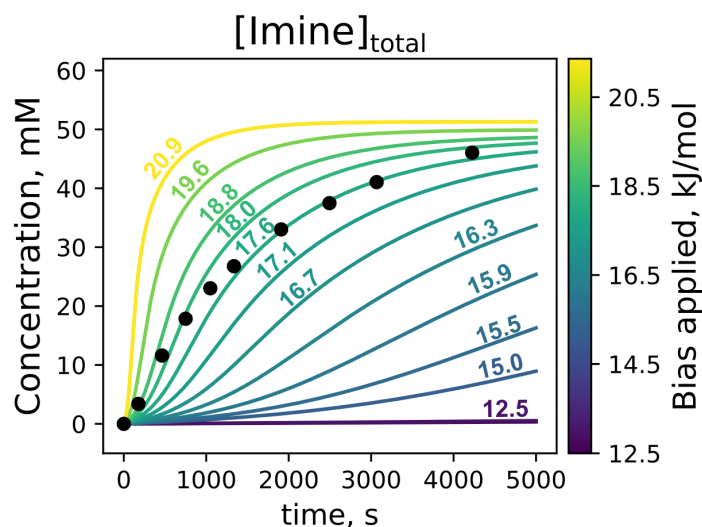

Figure 6: Total concentration of imine *vs* time of different microkinetic simulations upon constantly biased energies. The bias applied to each simulation is indicated in kJ/mol over the curve as well as in the colorbar legend. The experimental points are represented as black circles and were extracted from [66] following the procedure explained in our previous work [55].

With the resulting set of energies, we conducted a microkinetic simulation, which, revealing minimal imine formation, suggests the 13.38 kJ/mol correction transcends mere inaccuracies in electronic energy level cavity treatments. With the resulting set of energies we proceeded to run the microkinetic simulation. In our previous work we observed that upon the addition of other corrections, quasi-harmonic corrections, the concentration profile became completely incompatible with the experimental one, even when we followed the same approach and added a constant bias to the energy of each calculation. We decided to also apply it for the DRACO-corrected energies, the total concentration of imine is shown in **Figure 6**. To our surprise,

25

compared with our previous results, upon a correction of 17.56 kJ/mol the concentration profile showed an acceptable correlation with the experimental data. This may indicate that at least for this specific example, the correction introduced with DRACO is proportional to the molecularity of the species. Thus, it introduces a shift to the energies of each computed species that for our example is a negative value which leads to a higher correction. Next, we proceeded to visualize the concentration *vs* time evolution of the 17.56 kJ/mol corrected system using rNets, with the aim of getting more insights into significant changes in the reaction pathway to confirm the previous statement. **Figure 7a** and **b** show respectively the simplified network (comparable to **Figure 3)** at 10 mins and 40 mins respectively. The equivalent images with the full network can be found in the SI and a GIF with the evolution over time is also attached.

At 10 min, **Figure 7a**, the initial water (W) impurity is displaced towards forming an adduct ([N+W]) with the n-butylamine (N) which can act as a proton shuttle. As the concentration of n-butylamine and the benzaldehyde (A) the formation of the [A+N] adduct is very dynamic (showing a thicker reaction arrow) but as it is not thermodynamically favored it either reacts to form the hemiaminal or dissociates. As the reaction progresses, **Figure 7b**, the concentration of water increases as it is a product of the reaction, but instead of staying as an adduct with the imine (I) it is displaced to coordinate with the amine. As the amine is consumed more water is available increasing the formation of the [N+W+W] adduct, which is an intermediate in the water dimer ([W+W]) proton shuttle catalysis.
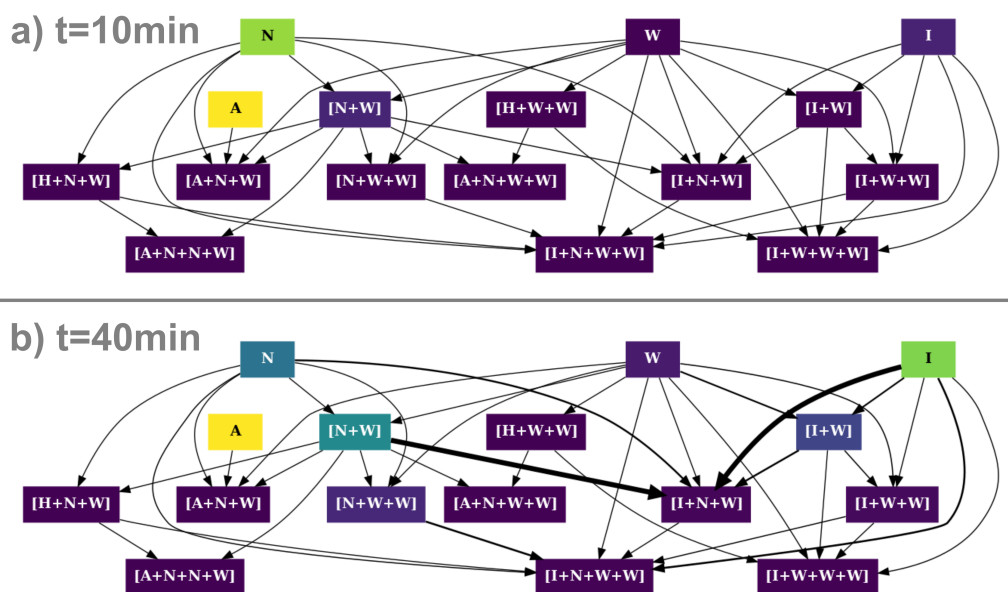
26

Figure 7: Simplified reaction network of the imine condensation in DCM between benzaldehyde and n-butylamine. The intermediates are labeled following the same nomenclature as in our previous work.[55] The thickness of the arrows represents the net rate for each elementary step, and the orientation of the arrow indicates the direction of the reaction, while the color of the nodes represents the concentration of the intermediates. A dark color represents a low or null concentration while a bright color corresponds to a high concentration.

3.2.2 CO_2 hydrogenation kinetics

Regarding the case study for heterogeneous systems, the analysis performed on the Pd(111) surface is confirmed with the kinetic utilities of rNets, as shown in **Figure 8**. The color of each node in **Figure 8** corresponds to the coverage at the steady state of each intermediate estimated through microkinetic simulations using AMUSE [49], performed assuming a differential Plug Flow Reactor (PFR) and the initial conditions were set to $P = 5 \cdot 10^6$ Pa, $T=573$K, and initial H_2:CO_2 ratio equals to 4, in line with the typical range of experimental operation conditions for CO_2 hydrogenation [56, 57]. The thickness of the edges (arrows) corresponds to the magnitude of the rate calculated with rNets from the coverages obtained with AMUSE of each elementary step, and the direction indicates whether the reaction is displaced to reactants or products. In **Figure 8**, it is clearly shown that all the kinetic equilibria are displaced to reactants and that only CO^* and $2H^*$ (i7 intermediate, $\theta_{i7} = 0.999$) is formed, poisoning the surface. This data supports quantitatively the qualitative analysis obtained with **Figure 4**. Thus, rNets has proven to be a useful tool not only for visualization but, more importantly, for the analysis of the results. In addition, rNets can be also used to follow a microkinetic simulation, as shown in the **Supporting Gif**, improving significantly the time and the analysis of the concentration profiles.
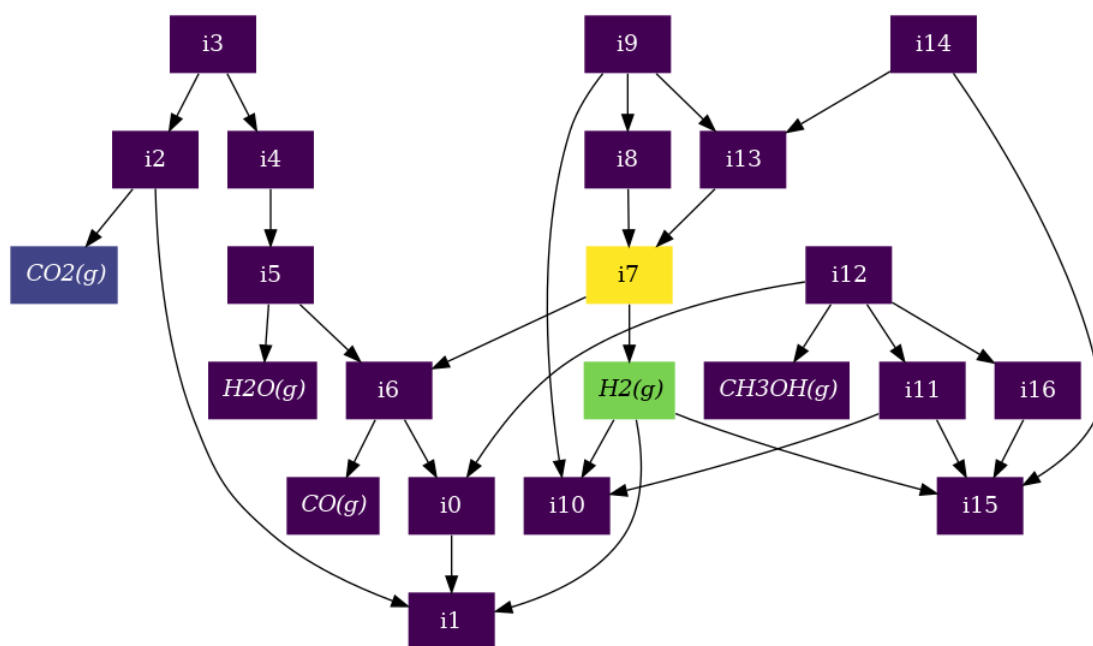
28

Figure 8: Visualization of the reaction network for CO_2 hydrogenation on Pd(111) considering the kinetic rates. The intermediates are labeled in **Table S3**. The thickness of the arrows represents the net rate for each elementary step, and the orientation of the arrow indicates the direction of the reaction, while the color of the nodes represents the concentration of the intermediates.

4 Conclusions

Through various application scenarios, rNets has proven to be a highly effective tool for the visualization of thermodynamic and kinetic properties within catalytic reaction networks. Its design is both minimalist and modular, ensuring straightforward integration with kinetic analysis software. This design choice offers users previews of reactions as well as comprehensive microkinetic analyses. Furthermore, rNets' user-friendly, table-based input system significantly reduces the learning curve, making it readily accessible even to chemists with limited programming expertise. As a pivotal advancement in open-source visualization tools for the chemistry sector, rNets exemplifies the power of simplifying the representation of complex data, thereby broadening its accessibility and utility in the community.

Data availability

The data used in this work is publicly available on the ioChem-BD platform.

- Imine condensation: geometry optimizations [https://doi.org/10.19061/iochem-bd-1-154] and single-point simulations [https://doi.org/10.19061/iochem-bd-1-308] with DRACO-based parameters.

- Regiospecific CO_2 fixation [https://doi.org/10.19061/iochem-bd-1-141].

- CO_2 hydrogenation on Pd(111) [https://doi.org/10.19061/iochem-bd-1-43].

https://doi.org/10.26434/chemrxiv-2024-l7gf5 **ORCID:** https://orcid.org/0000-0002-3327-9285 Content not peer-reviewed by ChemRxiv. **License:** CC BY 4.0

The input files and the intermediate dot files generated by rNets to build the figures of this work can be found as an examples in our code repository. Additionally, these examples have been integrated within the project documentation.

Code availability

The source code of rNets is publicly available at Github [https://github.com/spgarcica/rNets], including comprehensive documentation built with Sphinx [https://spgarcica.github.io/rNets.]

The source code of Pykinetic and AMUSE can be found on their respective Github repositories: [https://github.com/rperezsoto/pykinetic, https://github.com/LopezGroup-ICIQ/amuse]. Additionally, a package of Pykinetic can be found on PyPi [https://pypi.org/project/pykinetic/] and Zenodo [65]. The OntoRXN ontology [https://gitlab.com/dgarayr/ontorxn] and the Python library ontorxn-tools [https://gitlab.com/dgarayr/ontorxn_tools] to generate knowledge graphs are available on GitLab.

Acknowledgements

Author contributions

S. P.-G., conceptualization, methodology, software, writing - original draft, supervision, project administration. **R. P.-S.**, validation, investigation, data curation, writing - original draft, visualization. **A. S.-R.**, validation, investigation, data curation, writing - original draft, visualization. **D. G.-R.**, validation, investigation, data curation, writing - original draft, visualization. **V. N.**, conceptualization, methodology, software, writing review & editing. **N. L.**, writing review & editing, funding acquisition.

Competing interests statement

The authors declare no competing interests

32

References

(1) Chorkendorff, I., and Niemantsverdriet, J. W., *Concepts of Modern Catalysis and Kinetics*; Wiley: Weinheim, 2003, DOI: 10.1002/35276 02658.

(2) Salciccioli, M., Stamatakis, M., Caratzoulas, S., and Vlachos, D. G. (2011). A review of multiscale modeling of metal-catalyzed reactions: Mechanism development for complexity and emergent behavior. *Chem. Eng. Sci. 66*, 4319–4355.

(3) Mitchell, S., Vorobyeva, E., and Pérez-Ramírez, J. (2018). The multi-faceted reactivity of single-atom heterogeneous catalysts. *Angew. Chem. Int. Ed. 57*, 15316–15329.

(4) Ulissi, Z. W., Medford, A. J., Bligaard, T., and Nørskov, J. K. (2017). To address surface reaction network complexity using scaling relations machine learning and DFT calculations. *Nat. Commun. 8*, 14621.

(5) Margraf, J. T., Jung, H., Scheurer, C., and Reuter, K. (2023). Exploring catalytic reaction networks with machine learning. *Nat. Catal.*, 1–10.

(6) Pablo-García, S., García-Muelas, R., Sabadell-Rendón, A., and López, N. (2021). Dimensionality reduction of complex reaction networks in heterogeneous catalysis: From l inear-scaling relationships to statistical learning techniques. *WIREs Comput. Mol. Sci. 11*, e1540, DOI: 10.1 002/wcms.1540.

33

(7) Bruix, A., Margraf, J. T., Andersen, M., and Reuter, K. (2019). First-principles-based multiscale modelling of heterogeneous catalysis. *Nat. Catal. 2*, 659–670.

(8) Della Monica, F., and Kleij, A. W. (2020). Mechanistic Guidelines in Nonreductive Conversion of CO_2: The Case of Cyclic Carbonates. *Catal. Sci. Technol. 10*, 3483–3501, DOI: 10.1039/D0CY00544D.

(9) Kumar, A., Daw, P., and Milstein, D. (2022). Homogeneous Catalysis for Sustainable Energy: Hydrogen and Methanol Economies, Fuels from Biomass, and Related Topics. *Chem. Rev. 122*, 385–441, DOI: 10.1021/acs.chemrev.1c00412.

(10) Besora, M., and Maseras, F. (2018). Microkinetic Modeling in Homogeneous Catalysis. *Wiley Interdisciplinary Reviews: Computational Molecular Science 8*, 1–13, DOI: 10.1002/wcms.1372.

(11) Harvey, J. N., Himo, F., Maseras, F., and Perrin, L. (2019). Scope and Challenge of Computational Methods for Studying Mechanism and Reactivity in Homogeneous Catalysis. *ACS Catal. 9*, 6803–6813, DOI: 10.1021/acscatal.9b01537.

(12) Huang, R., Rintjema, J., González-Fabra, J., Martín, E., Escudero-Adán, E. C., Bo, C., Urakawa, A., and Kleij, A. W. (2019). Deciphering Key Intermediates in the Transformation of Carbon Dioxide into Heterocyclic Products. *Nature Catalysis 2*, 62–70, DOI: 10.1038/s41929-018-0189-z.

(13) Hueffel, J. A., Sperger, T., Funes-Ardoiz, I., Ward, J. S., Rissanen, K., and Schoenebeck, F. (2021). Accelerated Dinuclear Palladium Catalyst

34

Identification through Unsupervised Machine Learning. *Science 374*, 1134–1140, DOI: `10.1126/science.abj0999`.

(14) Nørskov, J. K., Rossmeisl, J., Logadottir, A., Lindqvist, L., Kitchin, J. R., Bligaard, T., and Jonsson, H. (2004). Origin of the overpotential for oxygen reduction at a fuel-cell cathode. *J. Phys. Chem. B 108*, 17886–17892.

(15) Frei, M. S., Mondelli, C., García-Muelas, R., Morales-Vidal, J., Philipp, M., Safonova, O. V., López, N., Stewart, J. A., Ferré, D. C., and Pérez-Ramírez, J. (2021). Nanostructure of nickel-promoted indium oxide catalysts drives selectivity in CO_2 hydrogenation. *Nat. Commun. 12*, 1960.

(16) Kaźmierczak, K., Ramamoorthy, R. K., Moisset, A., Viau, G., Viola, A., Giraud, M., Peron, J., Sicard, L., Piquemal, J.-Y., Besson, M., et al. (2020). Importance of the decoration in shaped cobalt nanoparticles in the acceptor-less secondary alcohol dehydrogenation. *Catal. Sci. Technol. 10*, 4923–4937, DOI: `10.1039/D0CY00390E`.

(17) Cannizzaro, F., Hensen, E. J., and Filot, I. A. (2023). The Promoting Role of Ni on In_2O_3 for CO_2 Hydrogenation to Methanol. *ACS Catal. 13*, 1875–1892.

(18) García-Muelas, R., and López, N. (2019). Statistical learning goes beyond the d-band model providing the thermochemistry of adsorbates on transition metals. *Nat. Commun. 10*, 4687.

(19) Pablo-García, S., Veenstra, F. L. P., Ting, L. R. L., García-Muelas, R., Dattila, F., Martín, A. J., Yeo, B. S., Pérez-Ramírez, J., and López,

35

N. (2022). Mechanistic routes toward C3 products in copper-catalysed CO_2 electroreduction. *Catal. Sci. Technol. 12*, 409–417, DOI: `10.1039/d1cy01423d`.

(20) Gupta, U., and Vlachos, D. G. (2020). Reaction Network Viewer (ReN-View): An open-source framework for reaction path visualization of chemical reaction systems. *SoftwareX 11*, 100442.

(21) Garay-Ruiz, D., Álvarez-Moreno, M., Bo, C., and Martínez-Núñez, E. (2022). New tools for taming complex reaction networks: the unimolecular decomposition of indole revisited. *ACS Phys. Chem. Au 2*, 225–236.

(22) Adobe Illustrator, `https://www.adobe.com`, Accessed: 2024-02-07.

(23) OriginLab, `https://www.originlab.com`, Accessed: 2024-02-07.

(24) Frei, M. S., Capdevila-Cortada, M., García-Muelas, R., Mondelli, C., López, N., Stewart, J. A., Ferré, D. C., and Perez-Ramirez, J. (2018). Mechanism and microkinetics of methanol synthesis via CO_2 hydrogenation on indium oxide. *J. Catal. 361*, 313–321, DOI: `10.1016/j.jcat.2018.03.014`.

(25) Inkscape, `https://inkscape.org`, Accessed: 2024-02-07.

(26) Pablo-García, S., Sabadell-Rendón, A., Saadun, A. J., Morandi, S., Pérez-Ramírez, J., and López, N. (2022). Generalizing Performance Equations in Heterogeneous Catalysis from Hybrid Data and Statistical Learning. *ACS Catal. 12*, 1581–1594, DOI: `10.1021/acscatal.1c04345`.

36

(27) Hunter, J. D. (2007). Matplotlib: A 2D graphics environment. *Comput. Sci. Eng. 9*, 90–95, DOI: `10.1109/MCSE.2007.55`.

(28) Garay-Ruiz, D., and Bo, C. (2021). Rationalizing the Mechanism of Peroxyformate Decomposition: Computational Insights To Understand Solvent Influence. *Chem. - Eur. J. 27*, 11618–11626, DOI: `10.1002/chem.202100755`.

(29) Petrus, E., Garay-Ruiz, D., Reiher, M., and Bo, C. (2023). Multi-Time-Scale Simulation of Complex Reactive Mixtures: How Do Polyoxometalates Form? *J. Am. Chem. Soc. 145*, 18920–18930, DOI: `10.1021/jacs.3c05514`.

(30) ChemDraw, `https://revvitysignals.com/products/research/chemdraw`, Accessed: 2024-02-07.

(31) Gansner, E. R., and North, S. C. (2000). An Open Graph Visualization System and Its Applications to Software Engineering. *Softw. Pract. Exper. 30*, 1203–1233.

(32) Li, Q., García-Muelas, R., and López, N. (2018). Microkinetics of Alcohol Reforming for H_2 Production From a Fair Density Functional Theory Database. *Nature Communications 9*, 526, DOI: `10.1038/s41467-018-02884-y`.

(33) Maeda, S., Ohno, K., and Morokuma, K. (2013). Systematic Exploration of the Mechanism of Chemical Reactions: The Global Reaction Route Mapping (GRRM) Strategy Using the ADDF and AFIR Methods. *Phys. Chem. Chem. Phys. 15*, 3683, DOI: `10.1039/c3cp44063j`.

37

(34) Maeda, S., Harabuchi, Y., Hayashi, H., and Mita, T. (2023). Toward Ab Initio Reaction Discovery Using the Artificial Force Induced Reaction Method. *Annu. Rev. Phys. Chem. 74*, 287–311, DOI: `10.1146/annurev-physchem-102822-101025`.

(35) Martínez-Núñez, E. (2015). An Automated Method to Find Transition States Using Chemical Dynamics Simulations. *J Comput Chem 36*, 222–234, DOI: `10.1002/jcc.23790`.

(36) Martínez-Núñez, E., Barnes, G. L., Glowacki, D. R., Kopec, S., Peláez, D., Rodríguez, A., Rodríguez-Fernández, R., Shannon, R. J., Stewart, J. J. P., Tahoces, P. G., and Vazquez, S. A. (2021). AUTOMEKIN2021 : An Open-source Program for Automated Reaction Discovery. *J Comput Chem 42*, 2036–2048, DOI: `10.1002/jcc.26734`.

(37) Kim, Y., Kim, J. W., Kim, Z., and Kim, W. Y. (2018). Efficient Prediction of Reaction Paths through Molecular Graph and Reaction Network Analysis. *Chem. Sci. 9*, 825–835, DOI: `10.1039/C7SC03628K`.

(38) Guan, Y., Ingman, V. M., Rooks, B. J., and Wheeler, S. E. (2018). AARON: An Automated Reaction Optimizer for New Catalysts. *J. Chem. Theory Comput. 14*, 5249–5261, DOI: `10.1021/acs.jctc.8b00578`.

(39) Wang, L.-P., Titov, A., McGibbon, R., Liu, F., Pande, V. S., and Martínez, T. J. (2014). Discovering Chemistry with an Ab Initio Nanoreactor. *Nature Chem 6*, 1044–1048, DOI: `10.1038/nchem.2099`.

(40) Unsleber, J. P., Grimmel, S. A., and Reiher, M. (2022). Chemoton 2.0: Autonomous Exploration of Chemical Reaction Networks. *J. Chem. Theory Comput. 18*, 5393–5409, DOI: `10.1021/acs.jctc.2c00193`.

(41) Vernuccio, S., and Broadbelt, L. J. (2019). Discerning complex reaction networks using automated generators. *AlChE J. 65*, e16663, DOI: `10.1002/aic.16663`.

(42) Goldsmith, C. F., and West, R. H. (2017). Automatic Generation of Microkinetic Mechanisms for Heterogeneous Catalysis. *Phys. Chem. C 121*, 9970–9981, DOI: `10.1021/acs.jpcc.7b02133`.

(43) Gao, C. W., Allen, J. W., Green, W. H., and West, R. H. (2016). Reaction Mechanism Generator: Automatic Construction of Chemical Kinetic Mechanisms. *Comput. Phys. Commun. 203*, 212–225, DOI: `10.1016/j.cpc.2016.02.013`.

(44) Hashemi, A., Bougueroua, S., Gaigeot, M.-P., and Pidko, E. A. (2022). ReNeGate: A Reaction Network Graph-Theoretical Tool for Automated Mechanistic Studies in Computational Homogeneous Catalysis. *J. Chem. Theory Comput. 18*, 7470–7482, DOI: `10.1021/acs.jctc.2c00404`.

(45) Chacko, R., Gossler, H., Angeli, S., and Deutschmann, O. (2023). Interconnected Digital Solutions to Accelerate Modeling of the Reaction Kinetics in Catalysis. *ChemCatChem*, e202301355.

(46) Álvarez-Moreno, M., de Graaf, C., López, N., Maseras, F., Poblet, J. M., and Bo, C. (2015). Managing the Computational Chemistry

Big Data Problem: The ioChem-BD Platform. *JCIM 55*, 95–103, DOI: 10.1021/ci500593j.

(47) Bo, C., Maseras, F., and López, N. (2018). The role of computational results databases in accelerating the discovery of catalysts. *Nat. Catal. 1*, 809–810.

(48) Garnier, S., Ross, N., Rudis, R., Camargo, A. P., Sciaini, M., and Scherer, C. viridis(Lite) - Colorblind-Friendly Color Maps for R, viridis package version 0.6.4, 2023, DOI: 10.5281/zenodo.4679423.

(49) Sabadell-Rendon, A., Kazmierczak, K., Morandi, S., Euzenat, F., Curulla-Ferre, D., and Lopez, N. (2023). Automated MUltiscale simulation environment. *Digital Discovery 2*, 1721–1732.

(50) Ryu, H., Park, J., Kim, H. K., Park, J. Y., Kim, S.-T., and Baik, M.-H. (2018). Pitfalls in Computational Modeling of Chemical Reactions and How To Avoid Them. *Organometallics 37*, Publisher: American Chemical Society, 3228–3239, DOI: 10.1021/acs.organomet.8b00456.

(51) Ribeiro, R. F., Marenich, A. V., Cramer, C. J., and Truhlar, D. G. (2011). Use of Solution-Phase Vibrational Frequencies in Continuum Models for the Free Energy of Solvation. *JPC B 115*, Publisher: American Chemical Society, 14556–14562, DOI: 10.1021/jp205508z.

(52) Luchini, G., Alegre-Requena, J. V., Funes-Ardoiz, I., and Paton, R. S. GoodVibes: automated thermochemistry for heterogeneous computational chemistry data, en, tech. rep. 9:291, Type: article, F1000Research, 2020, DOI: 10.12688/f1000research.22758.1.

(53) Jensen, F. (2024). Basis Set Superposition Errors Are Partly Basis Set Imbalances. *J. Chem. Theory Comput. 20*, Publisher: American Chemical Society, 767–774, DOI: `10.1021/acs.jctc.3c01156`.

(54) González-Fabra, J., Castro-Gómez, F., Sameera, W. M. C., Nyman, G., Kleij, A. W., and Bo, C. (2019). Entropic corrections for the evaluation of the catalytic activity in the Al(III) catalysed formation of cyclic carbonates from CO_2 and epoxides. *Catal. Sci. Technol. 9*, Publisher: The Royal Society of Chemistry, 5433–5440, DOI: `10.1039/C9CY012 85K`.

(55) Pérez-Soto, R., Besora, M., and Maseras, F. (2020). The Challenge of Reproducing with Calculations Raw Experimental Kinetic Data for an Organic Reaction. *Organic Letters 22*, Publisher: American Chemical Society, 2873–2877, DOI: `10.1021/acs.orglett.0c00367`.

(56) Alam, M. I., Cheula, R., Moroni, G., Nardi, L., and Maestri, M. (2021). Mechanistic and multiscale aspects of thermo-catalytic CO_2 conversion to C 1 products. *Catal. Sci. Technol. 11*, 6601–6629.

(57) Frei, M. S., Mondelli, C., García-Muelas, R., Kley, K. S., Puértolas, B., López, N., Safonova, O. V., Stewart, J. A., Curulla Ferré, D., and Pérez-Ramírez, J. (2019). Atomic-scale engineering of indium oxide promotion by palladium for methanol production via CO_2 hydrogenation. *Nat. Commun. 10*, 3377, DOI: `10.1038/s41467-019-11349-9`.

(58) Villagra-Soza, F., Godoy, S., Karelovic, A., and Jiménez, R. (2022). Scrutinizing the mechanism of CO_2 hydrogenation over Ni, CO and

41

bimetallic NiCo surfaces: Isotopic measurements, operando-FTIR experiments and kinetics modelling. *J. Catal. 414*, 1–15.

(59) Catapan, R. C., Oliveira, A. A., Chen, Y., and Vlachos, D. G. (2012). DFT study of the water–gas shift reaction and coke formation on Ni (111) and Ni (211) surfaces. *J. Phys. Chem. C 116*, 20281–20291.

(60) Dietz, L., Piccinin, S., and Maestri, M. (2015). Mechanistic Insights into CO_2 activation via reverse water–gas shift on metal surfaces. *J. Phys. Chem. C 119*, 4959–4966.

(61) Wilkinson, M. D. et al. (2016). The FAIR Guiding Principles for Scientific Data Management and Stewardship. *Sci Data 3*, 160018, DOI: `10.1038/sdata.2016.18`.

(62) Garay-Ruiz, D., and Bo, C. (2022). Chemical Reaction Network Knowledge Graphs : The OntoRXN Ontology. *J. Cheminform. 5*, 1–12, DOI: `10.1186/s13321-022-00610-x`.

(63) Maquilón, C., Limburg, B., Laserna, V., Garay-Ruiz, D., González-Fabra, J., Bo, C., Martínez Belmonte, M., Escudero-Adán, E. C., and Kleij, A. W. (2020). Effect of an Al(III) Complex on the Regio-and Stereoisomeric Formation of Bicyclic Organic Carbonates. *Organometallics 39*, 1642–1651, DOI: `10.1021/acs.organomet.9b00773`.

(64) Plett, C., Stahn, M., Bursch, M., Mewes, J.-M., and Grimme, S. (2024). Improving Quantum Chemical Solvation Models by Dynamic Radii Adjustment for Continuum Solvation (DRACO). *The Journal of Physical Chemistry Letters 15*, Publisher: American Chemical Society, 2462–2469, DOI: `10.1021/acs.jpclett.3c03551`.

42

(65) Pérez-Soto, R., Pablo-García, S., Besora, M., and Maseras, F. Pykinetic: v0.1.0, 2023, DOI: 10.5281/zenodo.8053050.

(66) Ciaccia, M., Cacciapaglia, R., Mencarelli, P., Mandolini, L., and Stefano, S. D. (2013). Fast transimination in organic solvents in the absence of proton and metal catalysts. A key to imine metathesis catalyzed by primary amines under mild conditions. *Chemical Science 4*, Publisher: The Royal Society of Chemistry, 2253–2261, DOI: 10.1039/C3SC50277E.